Toward Prediction of Alkane/Water Partition Coefficients

Anita Toulmin, J. Matthew Wood, and Peter W. Kenny*

AstraZeneca, Mereside, Alderley Park, Macclesfield, Cheshire SK10 4TG, United Kingdom

Received December 12, 2007

Partition coefficients were measured for 47 compounds in the hexadecane/water (P_{hxd}) and 1-octanol/water (P_{oct}) systems. Some types of hydrogen bond acceptor presented by these compounds to the partitioning systems are not well represented in the literature of alkane/water partitioning. The difference, ΔlogP, between $logP_{oct}$ and $logP_{hxd}$ is a measure of the hydrogen bonding potential of a molecule and is identified as a target for predictive modeling. Minimized molecular electrostatic potential (V_{min}) was shown to be an effective predictor of the contribution of hydrogen bond acceptors to ΔlogP. Carbonyl oxygen atoms were found to be stronger hydrogen bond acceptors for their electrostatic potential than heteroaromatic nitrogen or oxygen bound to hypervalent sulfur or nitrogen. Values of V_{min} calculated for hydrogen-bonded complexes were used to explore polarization effects. Predicted $logP_{hxd}$ and ΔlogP were shown to be more effective than $logP_{oct}$ for modeling brain penetration for a data set of 18 compounds.

Introduction

Lipophilicity is a fundamental physicochemical property in drug discovery[1–3] and is usually quantified by the logarithm of the 1-octanol/water partition coefficient[4] ($logP_{oct}$). Lipophilicity has been found to be an important determinant of permeability,[5] extent of penetration of drugs into cells and the central nervous system,[6] and volume of distribution.[7] Aqueous solubility[8,9] and binding to anti-targets such as the hERG[a] ion channel[10] are adversely influenced by lipophilicity and calculated $logP_{oct}$[11] ($ClogP_{oct}$) is frequently used as a molecular descriptor in predictive models for these properties. Lipinski's well-known rule of 5 warns of poor oral bioavailability if the $ClogP_{oct}$ of a compound exceeds 5.[1]

1-Octanol can form hydrogen bonds with solutes and water has a solubility of 2.5 M (equivalent to mole fraction of 0.29) in this solvent at 298 K.[12] It can be argued that these characteristics make 1-octanol a less appropriate model than hydrocarbon for the core of a membrane bilayer[13] or a hydrophobic binding pocket in a protein.[14] However, the poor solubility of many compounds in hydrocarbon solvents and volatility of some of these (e.g., cyclohexane) can present experimental difficulties. Molecules with both hydrogen bond donor and acceptor ability can also potentially self-associate[15] in the hydrocarbon phase, which may result in a concentration dependence of the measured partition coefficient.

Alkane/water partition coefficients (P_{alk}) are often compared with their 1-octanol/water equivalents and the difference ($logP_{oct} - logP_{alk}$) is termed ΔlogP.[16] This quantity is typically positive, and its magnitude reflects the strength of hydrogen bonding between solute and 1-octanol. It has been suggested that ΔlogP is a determinant of blood−brain barrier permeability in its own right.[17] It is worth noting that ΔlogP is effectively the 1-octanol/alkane partition coefficient and that the heptane/ethylene glycol system has also been used to assess solute hydrogen bonding.[18] Taylor and co-workers have devised a "critical quartet" of partitioning solvents, which includes donor and acceptor solvents in addition to inert alkane and amphiprotic 1-octanol.[19–21] A number of measured alkane/water partition coefficients have been reported in the literature for a variety of hydrocarbons including cyclohexane, 2,2,4-trimethylpentane (TMP), and hexadecane.[16,22–25] These partition coefficients were either measured directly or derived from measured values of gas solubility (Ostwald coefficient) in dry solvent.[23,24] Association of water and a polar solute in hydrocarbon will tend to increase the solubility of each in hydrocarbon, and the directly measured and derived partition coefficients are not necessarily equivalent.[26] Pharmaceutically relevant hydrogen bond acceptors such as heteroaromatic nitrogen and carbonyl oxygen are not well represented in the literature of alkane/water partitioning, and hydrogen bond donors are rarely found in the absence of acceptors.

Counting hydrogen bond donors and acceptors is a recurring theme in computer-aided drug discovery. A molecule violates the rule of 5 if it has more than 10 hydrogen bond acceptors (oxygen or nitrogen atoms) or 5 donors (acceptors with at least one directly bonded hydrogen atom).[1] It is significant that the rule of 5 defines the lower lipophilicity limit for oral bioavailability in terms of hydrogen bonding rather than partition or distribution coefficients. Polar surface area (PSA)[27] is effectively a count of atoms capable of hydrogen bonding with weighting for solvent exposure and is often calculated directly from the molecular connection table[28,29] without using a 3D structural model. It can be argued that data analytic approaches based on counting hydrogen bond donors and acceptors would benefit from a more quantitative model of hydrogen bonding, especially if it brought donors and acceptors onto the same scale.

Equilibrium constants measured in nonpolar solvents have been used to quantify hydrogen bond strength, typically using a standard donor to quantify acceptors and standard acceptor

* To whom correspondence should be addressed. Phone: +44 1625 514396. Fax: +44 1625 519749. E-mail: pwk.pub.2008@gmail.com.

[a] Abbreviations: B3LYP, Becke three-parameter exchange functional with Lee−Yang−Parr correlation functional; BBB, blood-brain barrier; C_{blood}, concentration of drug in blood; C_{brain}, concentration of drug in brain; ClogP, calculated logarithm of 1-octanol/water partition coefficient; CNS, central nervous system; *D*, distribution coefficient; D_{hxd}, hexadecane/water distribution coefficient; D_{oct}, 1-octanol/water distribution coefficient; DMSO, dimethylsulfoxide; hERG, human ether-a-go-go related gene; HPLC, high performance liquid chromatography; MP2, second-order Møller−Plesset perturbation theory; P_{alk}, alkane/water partition coefficient; P_{hxd}, hexadecane/water partition coefficient; P_{oct}, 1-octanol/water partition coefficient; PSA, polar surface area; QSPR, quantitative structure property relationship; RHF, restricted Hartree−Fock; rms, root-mean-square; TMP, 2,2,4-trimethylpentane; V_{min}, minimized electrostatic potential; ΔlogP, difference between $logP_{oct}$ and $logP_{hxd}$; $\Delta logP_{meas}$, measured ΔlogP; $\Delta logP_{mep}$, contribution to ΔlogP predicted from molecular electrostatic potential; $\Delta logP_{pred}$, predicted ΔlogP; $\Delta logP_{ss}$ contribution to ΔlogP predicted from substructure.

10.1021/jm701549s CCC: $40.75
Published on Web 06/18/2008

for donors.[30–32] The stability of the 1−1 complex is measured and, for molecules with more than one hydrogen bonding group, the equilibrium constant is a sum of equilibrium constants for all such complexes. Only a single intermolecular hydrogen bond is typically present in each complex although specific features such as the carboxylic acid or primary amide may allow additional hydrogen bonds to form. The situation in a solvent capable of hydrogen bonding, in which all donors and acceptors are simultaneously exposed to solvent molecules, is quite different.[21] Nevertheless, hydrogen bond donor and acceptor strengths measured for 1−1 complexes are still useful for modeling solvation.[33] Electrostatic potential calculated using quantum mechanical models has been found to be a useful predictor of hydrogen bond donor and acceptor strengths.[34–36] Hydrogen bond acceptors are typically associated with one or two electrostatic potential minima at which the electric field vanishes. The value, V_{min}, of the potential at the minimum has been found to be a particularly effective predictor of hydrogen bond acceptor strength.[34–36] These quantitative structure property relationships (QSPRs) are typically derived using model compounds, each of which has only a single hydrogen bonding group, because the thermodynamic measurements do not in general allow contributions of individual equilibria to be quantified.

In this study, we present measured hexadecane/water and 1-octanol/water partition coefficients for a number of compounds and use these to evaluate minimized electrostatic potential as a predictor of ΔlogP. We believe that meaningful, directly measured, alkane/water partition coefficients will simply not be accessible for many compounds of pharmaceutical interest and that predictive methods will be necessary to provide this information. The 1-octanol/water partition coefficient is measured routinely in pharmaceutical research laboratories and provides a convenient starting point for prediction of its alkane/water equivalent. This approach identifies ΔlogP as a target for predictive modeling and focuses on hydrogen bond acceptors that will be neutral under normal physiological conditions. The model compounds have been selected to present a number of relevant functional groups to the partitioning systems. The observed relationships between ΔlogP and V_{min} have implications beyond their application to prediction of ΔlogP.

Measured Partition Coefficients

Distribution coefficients for the hexadecane/water (D_{hxd}) and 1-octanol/water (D_{oct}) systems were measured (Table 1) at a pH of 7.4 for a number of compounds (Figure 1). The most basic of these (**7**) has a pK_a of 6.7,[37] so, for this work, logD and logP are equivalent. As our focus is on ΔlogP, it would still be valid to derive this from $logD_{oct} - logD_{hxd}$ for compounds that are predominantly ionized in the aqueous phase, provided that no ionized species partition into either organic phase. Most of the compounds were selected on the basis of having a single hydrogen bond acceptor (e.g., **1**) or two symmetrically equivalent acceptors (e.g., **6**, **38**) while lacking donors although two compounds (**43**, **44**), each with a single donor and lacking acceptors were also assayed. Compatibility with HPLC-UV detection and likelihood of the measured value falling outside the routine limits of the assay were additional factors in selection of compounds for measurement. Values of $logD_{hxd}$ measured in this study were consistent with 2,2,4-trimethylpentane/water logP measurements[22] reported for **1** (−0.41), **12** (2.03), **14** (1.12), **40** (1.43), and **41** (0.99) and $logP_{hxd}$ values derived from gaseous solubility[24] for **1** (−0.42), **12** (2.13), **14** (1.12), **40** (1.44), and **41** (0.99).

Table 1. Measured Hexadecane/Water and 1-Octanol/Water Partition Coefficients

structure	$logD_{oct}$	SE ($logD_{oct}$)[a]	$logD_{hxd}$	SE ($logD_{hxd}$)[b]	ΔlogP[c]	V_{min}[d,e]
1	0.64	0.005	−0.48	0.023	1.12	−0.1129
2	1.23	0.005	0.52	0.019	0.71	−0.0983
3	1.99	0.030	0.97	0.087	1.02	−0.1101
4	2.09	0.031	0.98	0.003	1.11	−0.1128
5	1.31	0.015	0.47	0.007	0.84	−0.0933
6	0.79	0.085	−0.49	0.019	1.28	−0.1021
7	1.55	0.017	−0.83	0.035	2.38	−0.1305
8	1.34	0.013	−0.89	0.019	2.23	−0.1219
9	1.56	0.034	0.89	0.017	0.67	−0.0998
10	1.97	0.009	1.25	0.044	0.73	−0.0969
11	1.49	0.025	0.75	0.026	0.74	−0.1021
12	2.15	0.006	1.90	0.095	0.25	−0.0712
13	1.74	0.000	1.36	0.026	0.38	−0.0925
14	1.61	0.020	0.96	0.046	0.65	−0.0921
15	0.71	0.009	−0.98	0.042	1.68	−0.1076
16	1.00	0.043	−0.54	0.023	1.54	−0.1093
17	1.83	0.012	0.07	0.020	1.76	−0.1071
18	1.32	0.005	−0.60	0.025	1.92	−0.1098
19	1.25	0.003	0.00	0.015	1.25	−0.0997
20	1.69	0.012	0.49	0.015	1.20	−0.1003
21	0.87	0.009	−1.07	0.094	1.93	−0.1071
22	1.32	0.065	−0.15	0.042	1.47	−0.0993
23	1.33	0.035	0.53	0.010	0.80	−0.0798
24	1.60	0.010	0.16	0.019	1.44	−0.1064
25	1.37	0.015	−0.72	0.036	2.09	−0.1121
26	2.09	0.006	−0.03	0.006	2.12	−0.1069
27	2.47	0.003	0.18	0.015	2.28	−0.1053
28	1.52	0.059	−0.15	0.015	1.67	−0.1080
29	2.47	0.013	−1.76	0.040	4.23	−0.1262
30	1.80	0.013	−1.40	0.040	3.20	−0.1149
31	1.02	0.007	−0.29	0.024	1.31	−0.1037
32	1.44	0.023	0.34	0.003	1.10	−0.1006
33	1.90	0.012	0.56	0.009	1.34	−0.1017
34	3.49	0.020	1.99	0.025	1.50	−0.1046
35	1.71	0.019	−0.57	0.059	2.28	−0.1259
36	2.10	0.009	0.66	0.007	1.45	−0.1174
37	2.81	0.003	1.23	0.027	1.57	−0.1223
38	2.41	0.033	0.75	0.057	1.65	−0.0942
39	2.20	0.038	1.12	0.025	1.08	−0.0971
40	1.83	0.013	1.35	0.021	0.48	−0.0781
41	1.56	0.009	0.91	0.010	0.65	−0.0922
42	1.75	0.006	0.92	0.003	0.83	−0.0965
43	2.24	0.005	0.66	0.025	1.58	
44	3.22	0.044	1.36	0.029	1.86	

[a] Standard error for mean $logD_{oct}$. [b] Standard error for $logD_{hxd}$. [c] Calculated before rounding logD to to 2 decimal places. [d] Most negative minimum when two or more V_{min} values are associated with a single atom. [e] In atomic units (Hartree/electron).

Relationships between ΔlogP and Minimized Electrostatic Potential

Values of ΔlogP calculated from $logD_{oct} - logD_{hxd}$ were used to explore the utility of V_{min} as a descriptor of hydrogen bond acceptor strength and predictor of ΔlogP. Plotting the results from Table 1 suggested that the acceptors fell into three classes: (1) doubly connected heteroaromatic nitrogen, nitrile nitrogen, or ether oxygen, (2) carbonyl oxygen, and (3) oxygen singly connected to hypervalent atom. Consequently, separate analyses were performed for each class of acceptor.

Contributions of hydrogen acceptors to ΔlogP are assumed to be additive, and measured values for compounds such as **5**, **6**, **22**, **38**, and **39** with two equivalent acceptors were statistically corrected prior to analysis. Plots of statistically corrected ΔlogP against V_{min} are shown in Figures 2–4 for the three classes of acceptors. Comparison of Figures 2 and 3 shows a carbonyl

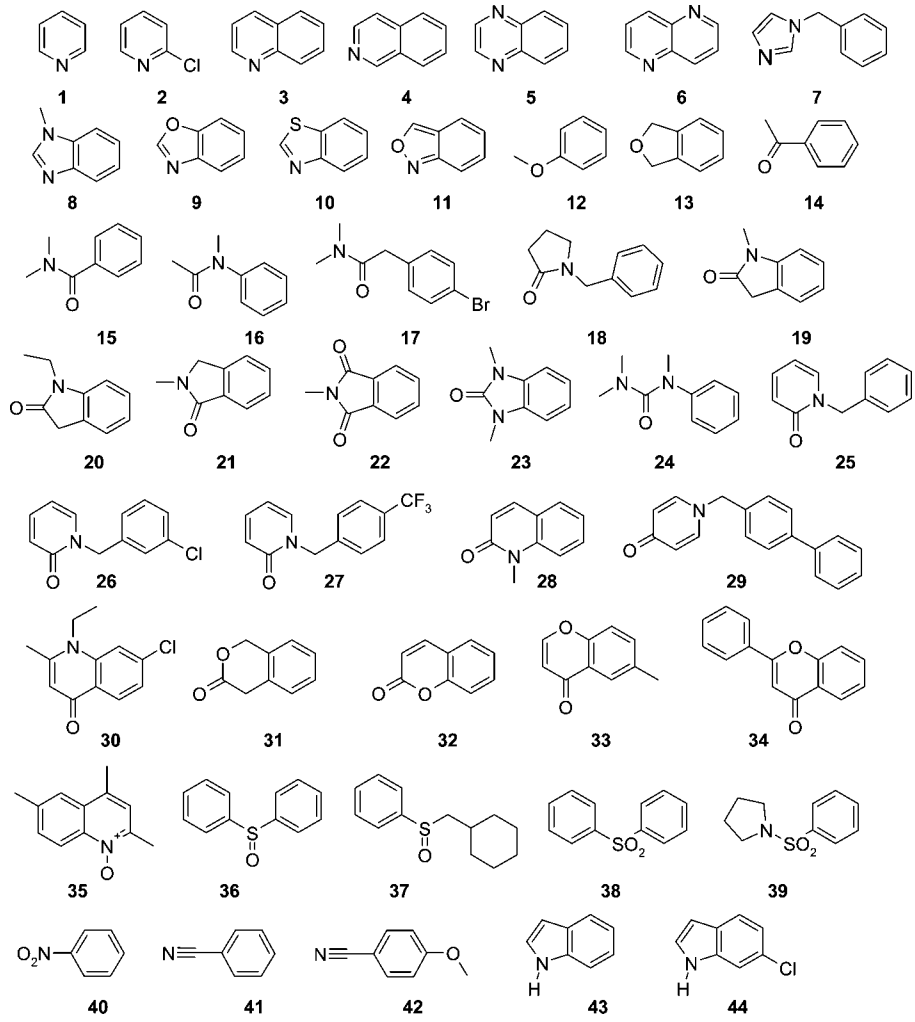

Figure 1. Structures of compounds for which $logP_{hxd}$ and $logP_{oct}$ were measured.

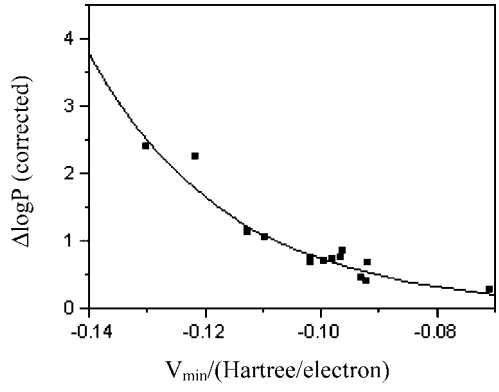

Figure 2. Plot of ΔlogP (statistically corrected for number of acceptors) against minimized electrostatic potential (RHF/6-31G*; atomic units) for heteroaromatic nitrogen, nitrile nitrogen, and ether oxygen acceptors.

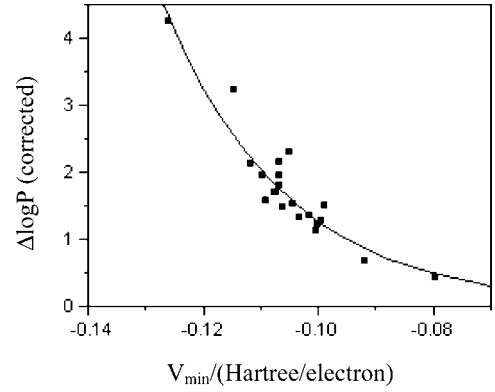

Figure 3. Plot of ΔlogP (statistically corrected for number of acceptors) against minimized electrostatic potential (RHF/6-31G*; atomic units) for carbonyl oxygen acceptors.

oxygen atom to be a stronger hydrogen bond acceptor than an aromatic nitrogen atom with the same V_{min} value. This is probably a consequence of using only a single electrostatic potential minimum to model the carbonyl oxygen acceptors when both oxygen lone pairs are likely to participate in hydrogen bonding. While the curves in Figures 3 and 4 are reasonably similar, the data sets have not been combined because of the differing numbers of lone pairs associated with these two classes of acceptor. Fitting a linear model to these data sets showed clear systematic error with large positive residuals at the extremes and negative residuals at the near the mean for V_{min}. Similar curvature has been observed in plots of hydrogen bond acceptor strength against V_{min}.[34,35] An additional disadvantage of the linear model is that it predicts that ΔlogP will become negative for very weak acceptors rather than tending to zero as is normally observed. Equation 1 was used to model the experimental data because it leads to a good fit for each class of acceptor (Figures 2–4) while using the same number of

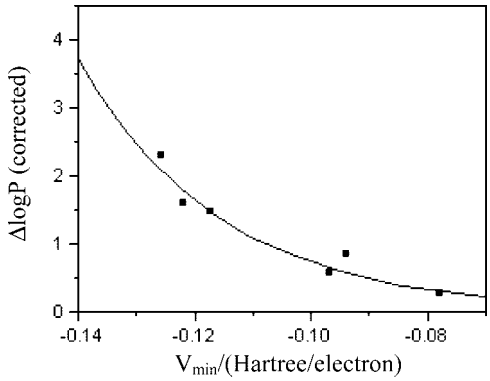

Figure 4. Plot of ΔlogP (statistically corrected for number of acceptors) against minimized electrostatic potential (RHF/6-31G*; atomic units) for singly connected oxygen acceptors linked to hypervalent sulfur or nitrogen.

Table 2. Fit of eq *1* to ΔlogP For Different Classes of Acceptor and Levels of Theory

eq	acceptor type	theoretical model[a]	$\Delta\log P_0 \times 10^2$	k^b	RMSE [c]
1a	heteroaromatic and nitrile N; ether O	RHF/6-31G*	1.14	41.5	0.17
1b	heteroaromatic and nitrile N; ether O	B3LYP/6-31G*	1.20	45.4	0.16
1c	heteroaromatic and nitrile N; ether O	MP2/6-31G*	1.40	42.5	0.18
1d	carbonyl O	RHF/6-31G*	1.08	47.6	0.29
1e	carbonyl O	B3LYP/6-31G*	2.00	48.1	0.30
1f	carbonyl O	MP2/6-31G*	2.25	47.7	0.33
1g	O singly connected to hypervalent N or S	RHF/6-31G*	1.22	40.8	0.21
1h	O singly connected to hypervalent N or S	B3LYP/6-31G*	1.23	50.2	0.37
1i	O singly connected to hypervalent N or S	MP2/6-31G*	2.22	44.0	0.41

[a] Using molecular geometry energy-minimized at RHF/6-31G* level of theory. [b] In atomic units (Hartree/electron)$^{-1}$. [c] Root mean square error.

parameters as the linear model and has the desired asymptotic behavior at high V_{min}.

$$\Delta\log P = \Delta\log P_0 \times e^{-kV_{min}} \quad (1)$$

The V_{min} values used to fit ΔlogP in Figures 2–4 were calculated at the restricted Hartree−Fock (RHF)[38] level of theory because this resulted in the best fit to the experimental results across all three classes of acceptor. Second-order Møller−Plesset perturbation theory (MP2)[38] and the B3LYP[39] hybrid density functional both led to worse fitting of the experimental data for oxygen acceptors (class 2 and 3) when used to calculate V_{min} (Table 2). The three theoretical models perform similarly for the class 1 acceptors (heteroaromatic nitrogen, nitrile nitrogen, ether oxygen), although using the B3LYP[39] model does result in a slightly lower rms error than using the RHF[38] model. Differences in performance between the RHF and B3LYP models are minimal for the class 1 and 2 acceptors.

These models for ΔlogP allow the contribution of each acceptor to be quantified individually. While measured values for compounds with non-equivalent acceptors are less easily used for deriving models, it has been shown that these are still useful for validation.[36] A validation set (Figure 5, Table 3) was created from our measured values for three heterocycles with nonequivalent hydrogen bond acceptors and a number of results from the literature. The predicted value of ΔlogP for the phosphine oxide **61** is 0.8 units less than the measured value, suggesting that this type of hydrogen bond acceptor will require special treatment within this framework. Other than that, the three largest differences between measured and predicted ΔlogP are observed for **58** (0.40; from TMP/water partition coefficient[22]), **49** (0.41; this work), and **57** (0.43; from derived hexadecane/water partition coefficient[24]).

Polarization Effects

Minimized electrostatic potential was used to explore the effect of polarization using methanol as a model for 1-octanol. Polarization effects are quantified by comparing corresponding values of V_{min} for complexes with methanol and the uncomplexed acceptors. Three structures (Figure 5) were chosen to span a wide range in V_{min} and to have carbonyl groups with symmetrically equivalent electrostatic potential minima. The results, which also show the effects of complex formation on the V_{min} values associated with methanol oxygen, are presented in Table 4.

CNS Penetration

Measured and predicted contributions of hydrogen bonding groups to ΔlogP were used to estimate this quantity for compounds with known ability to penetrate the CNS. Estimates for ΔlogP were derived by summing fragment contributions defined substructurally ($\Delta\log P_{ss}$) and those predicted from computed molecular electrostatic potential ($\Delta\log P_{mep}$). Values of $\Delta\log P_{ss}$ were derived using the measured values presented in this study (e.g., aliphatic tertiary amide: 1.8; alkyl aryl ether: 0.2) or by analysis of values reported in the literature (e.g., aliphatic alcohol: 1.6; dialkylamine: 1.0). The effect of self-association was neglected in defining $\Delta\log P_{ss}$ for hydroxyl groups and secondary amine nitrogen. The contribution of intramolecular hydrogen bonds to ΔlogP was also neglected, and this can be justified by noting that the measured $\Delta\log P_{ss}$ of 2-ethoxyethanol (1.9)[25] is well predicted by the sum of our $\Delta\log P_{ss}$ for aliphatic hydroxyl (1.6) and the measured $\Delta\log P_{ss}$ value for **52** (0.3, Table 3).

The calculations for prediction of $\log P_{hxd}$ from measured values[40] of $\log P_{oct}$ are illustrated in detail for morphine (**64**) and diamorphine (**65**) in Table 5. Values of $\log P_{hxd}$ and ΔlogP predicted using the same methodology are presented in Table 6 for 18 compounds (Figure 6) for which measured brain/blood concentration ratios (C_{brain}/C_{blood}) have been reported in the literature.[41] The plots of $\log(C_{brain}/C_{blood})$ against predicted $\log P_{oct}$ (Figure 7, $R^2 = 0.66$; RMSE = 0.54) and predicted $\log P_{hxd}$ (Figure 8; $R^2 = 0.82$; rms error = 0.39) show the latter to be a better predictor of CNS penetration for this data set. The difference between observed and predicted $\log(C_{brain}/C_{blood})$ for **78** is larger when the data is fit with $\log P_{oct}$ (1.74) than with $\log P_{hxd}$ (1.22). The plot of $\log(C_{brain}/C_{blood})$ against $\Delta\log P_{pred}$ (Figure 9, $R^2 = 0.88$; RMSE = 0.32) shows this property to be a more effective predictor than $\log P_{hxd}$ for CNS penetration.

Discussion

The primary motivation for this study is to gain better access to alkane/water partition coefficients. We have chosen $\log P_{oct}$ as our starting point because it is measured routinely in pharmaceutical research, a substantial body of measured data is available,[42] and methods have been developed for its prediction.[11] Alkane and 1-octanol are the inert and amphiprotic components of the "critical quartet",[19] and it can be argued that either of the other two components (chloroform, propylene glycol dinonoate) would be better starting points for prediction on the grounds that their interactions with polar solutes are likely

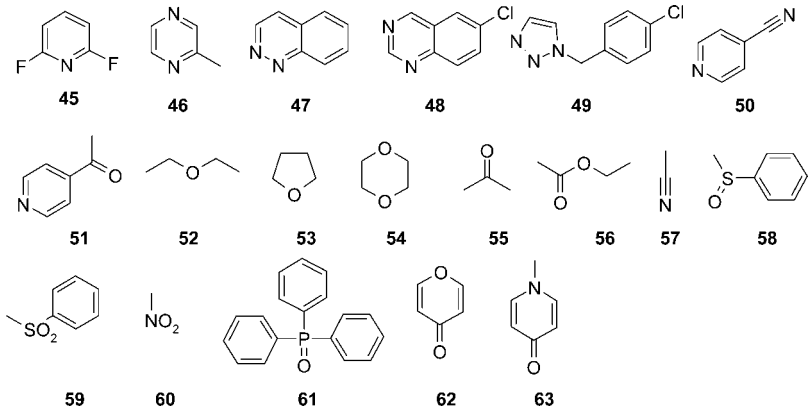

Figure 5. Structures of compounds used to validate models for ΔlogP and study polarization effects.

Table 3. Comparison of Measured and Predicted ΔlogP Values For Validation Set

structure	$\log P_{oct}$ [a]	$\log P_{alk}$	$\Delta\log P_{meas}$	$\Delta\log P_{pred}$	V_{min} [b]
45	1.17	0.89[c]	0.28	0.42	−0.0869
46	0.23	−0.79[d]	1.02	1.26	
				0.62 (N1)	−0.0962 (N1)
				0.64 (N4)	−0.0973 (N4)
47	1.01(0.02)[e]	−0.74 (0.02)[e]	1.75	2.04	
				0.93 (N1)	−0.1062 (N1)
				1.11 (N2)	−0.1105 (N2)
48	1.78(0.01)[e]	0.80 (0.01)[e]	0.98	1.11	
				0.55 (N1)	−0.0935 (N1)
				0.56 (N3)	−0.0940 (N3)
49	1.78(0.03)[e]	−0.27 (0.02)[e]	2.05	1.64	
				0.42 (N2)	−0.0873 (N2)
				1.22 (N3)	−0.1128 (N3)
50	0.46	−0.59[c]	1.05	0.80	
				0.48 (N1)	−0.0901 (N1)
				0.32 (CN)	−0.0803 (CN)
51	0.48	−0.93[c]	1.51	1.30	
				0.81 (N)	−0.1027 (N)
				0.49 (O)	−0.0801 (O)
52	0.89	0.62[f]	0.27	0.46	−0.0890
53	0.46	−0.02[g]	0.48	0.69	−0.0988
54	−0.27	−0.81[d]	0.54	0.78	−0.0855
55	−0.24	−1.03[g]	0.79	0.85	−0.0917
56	0.73	0.22[g]	0.51	0.84	−0.0915
57	−0.34	−1.29[g]	0.95	0.52	−0.0921
58	0.55	−1.49[h]	2.04	1.64	−0.1200
59	0.50	−0.92[h]	1.42	1.11	−0.0934
60	−0.35	−1.06[g]	0.71	0.52	−0.0748
61	2.83	0.25 (0.05)[e]	2.58	1.77	−0.1218

[a] Reference 42 unless indicated otherwise. [b] Most negative minimum when two or more V_{min} values are associated with a single atom; atomic units (Hartree/electron). [c] "Alkane" value; ref 25. [d] Hexadecane obtained indirectly from gaseous solubility measurement; ref 25. [e] This work; standard error in parenthesis. [f] Hexadecane; ref 19. [g] Hexadecane obtained indirectly from gaseous solubility measurement; ref 24. [h] 2,2,4-Trimethylpentane; ref 22.

Table 4. Polarization Effects For Carbonyl Oxygen Acceptor and Methanol Donor

structure	V_{min} (O=C) [a]	$\Delta\log P_{pred}$ (O=C) [b]	V_{min} (O=C) complex	V_{min} (MeOH) complex [a,c]
55	−0.0917	0.85	−0.0782	−0.1134
62	−0.1029	1.45	−0.0920	−0.1149
63	−0.1251	4.15	−0.1137	−0.1266

[a] Atomic units (Hartree/electron) [b] From eq 1d (Table 2). [c] Compare with −0.0966 for isolated methanol molecule.

to be less complex than the interactions of 1-octanol with these solutes. However, these solvents are used too rarely in partitioning systems to be viable starting points for prediction of $\log P_{alk}$. We assume that individual contributions of hydrogen bond donors and acceptors to ΔlogP are additive and show that

Table 5. Partition Coefficients and Calculated Polar Surface Areas For Morphine and Diamorphine[e]

structure	PSA/Å^2	$\log P_{oct}$ [a]	ΔlogP contributions	$\Delta\log P_{pred}$	predicted $\log P_{hxd}$
64	52.9	0.89	0.8 [b] (tertiary amine)	5.1	−4.2
			2.5 [b] (phenol)		
			1.6 [b] (alcohol)		
			0.2 [b,c] (ether)		
65	65.1	1.58	0.8 [b] (tertiary amine)	3.0	−1.4
			1.0 [d] (aryl ester)		
			1.0 [d] (alkyl ester)		
			0.2 [b,c] (ether)		

[a] Measured value from ref 40. [b] $\Delta\log P_{ss}$. [c] This work. [d] $\Delta\log P_{ss}$ from eq 1d. [e] From $\log P_{oct} - \Delta\log P_{pred}$.

Table 6. Measured Brain/Blood Ratios and Predicted Partition Coefficients For Analysis of CNS Penetration

compound	$\log (C_{brain}/C_{blood})$[a]	ClogP[b]	$\Sigma\Delta\log P_{ss}$[c]	$\Sigma\Delta\log P_{mep}$[d]	$\Delta\log P_{pred}$[e]	$\log P_{hxd}$[f]
66	1.00	4.47	1.0 [g]	0.0	1.0	3.5
67	1.05	5.04	0.8 [h]	0.0	0.8	4.2
68	0.99	3.76	0.8 [h]	0.0	0.8	3.0
69	0.98	4.85	0.8 [h]	0.0	0.8	3.5
70	0.82	3.82	2.4 [h,i]	0.1	2.5	1.3
71	0.52	3.31	2.6 [g,i]	0.1	2.7	0.6
72	1.03	4.58	0.8 [h]	0.1	0.9	3.7
73	0.39	4.13	1.0 [g]	0.1	1.1	3.0
74	0.53	2.81	0.8 [h]	1.0	1.8	1.0
75	0.49	3.22	1.0 [h,j]	0.8	1.8	1.4
76	−0.02	2.71	0.8 [h]	2.6	3.4	−0.7
77	−0.67	1.07	2.4 [h,i]	2.6	5.0	−3.9
78	1.64	2.21	1.0 [g]	0.3	1.3	0.9
79	−0.02	2.61	2.6 [h,i,j]	0.0	2.6	0.0
80	−0.30	2.57	0.0	3.6	3.6	−1.0
81	−1.34	1.05	1.6 [i]	3.6	5.2	−4.1
82	−1.82	−0.16	3.2 [i]	3.6	6.8	−7.0
83	0.16	2.09	2.6 [h,k]	0.5	3.1	−1.0

[a] Ref 41. [b] Ref 11. [c] Summed substructural fragment contributions to ΔlogP. [d] Summed contributions to ΔlogP calculated from molecular electrostatic potential. [e] Predicted ΔlogP. [f] Predicted hexadecane/water partition coefficient. [g] $\Delta\log P_{ss}$ for dialkylamine: 1.0. [h] $\Delta\log P_{ss}$ for trialkylamine: 0.8. [i] $\Delta\log P_{ss}$ for aliphatic alcohol: 1.6. [j] $\Delta\log P_{ss}$ for alkoxyphenyl: 0.2. [k] $\Delta\log P_{ss}$ for aliphatic tertiary amide: 1.8.

calculated electrostatic potentials are predictive of these contributions. There is an analogy between this focus on ΔlogP and the free energy perturbation method[43] and matched molecular pair analysis[44,45] in that changes in a property may be more easily predicted than the property itself. Robust prediction of ΔlogP coupled with routine measurement of $\log P_{oct}$ would clearly lead to $\log P_{alk}$ prediction. We suggest that, in some situations, $\log P_{alk}$ may prove to be a more suitable descriptor than $\log P_{oct}$ in predictive models for physicochemical properties and physiological processes. One criterion by which suitability

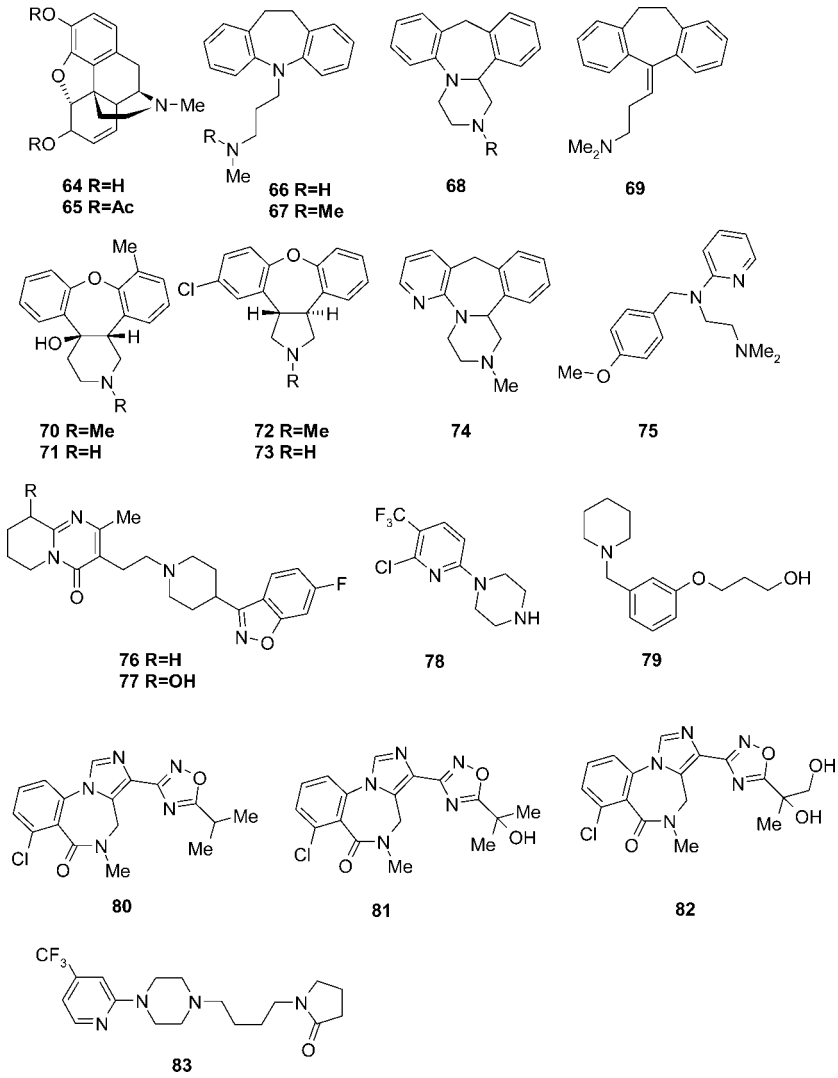

Figure 6. Structures of compounds used in analysis of CNS penetration.

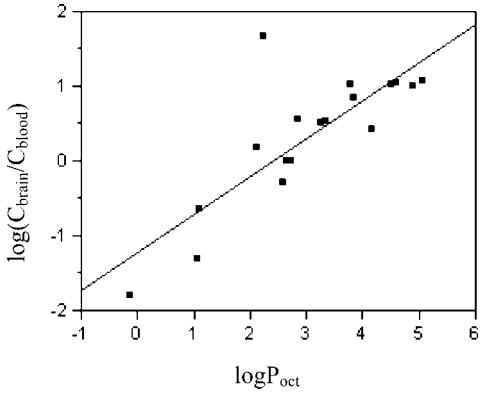

Figure 7. Plot of brain/blood concentration ratio against predicted 1-octanol/water partition coefficient ($N = 18$; $R^2 = 0.66$; RMSE = 0.54; intercept = −1.22; slope = 0.51).

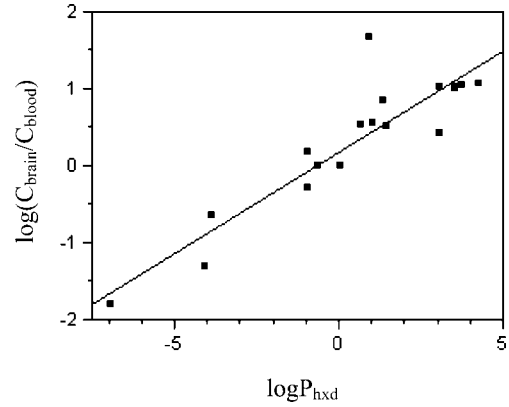

Figure 8. Plot of brain/blood concentration ratio against predicted hexadecane/water partition coefficient ($N = 18$; $R^2 = 0.82$; RMSE = 0.39; intercept = 0.18; slope = 0.26).

might be judged is whether a lower limit of lipophilicity for bioavailability can be defined in terms of partition or distribution coefficient rather than numbers of hydrogen bonding groups.

The measured ΔlogP values presented here represent a number of the neutral hydrogen bond acceptors that are encountered in medicinal chemistry. The most striking result is the ΔlogP of 4.23 (PSA = 22.0 Å^2) for the 4-pyridone **29**, which, despite minimal differences in PSA, is significantly greater than any of those measured for the 2-pyridones **25**, **26**, and **27** (2.09−2.28). The ΔlogP of 3.2 measured for the 4-quinolone **30** shows the carbonyl oxygen to be a strong acceptor, a characteristic that is also reflected in the unusually high pK_a values that are observed for the 3-carboxylate group in quinolone antibiotics.[46] The nitro group contributes 3 acceptors in the application of the rule of 5 and has a relatively large PSA of 45.8 Å^2 although the ΔlogP of 0.48 measured for

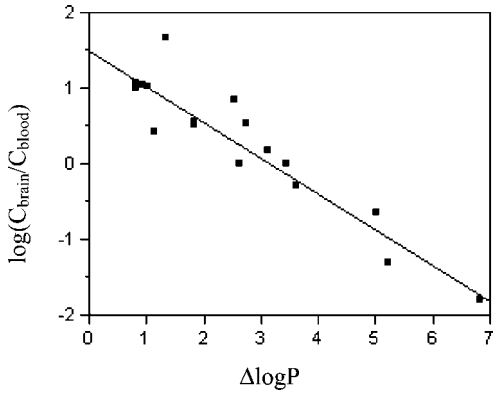

Figure 9. Plot of brain/blood concentration ratio against predicted ΔlogP ($N = 18$; $R^2 = 0.88$; RMSE = 0.32; intercept = 1.49; slope = −0.47).

40 suggests weak hydrogen bonding. Comparison of **23** (ΔlogP =1.47, PSA = 26.9 Å^2) and **22** (ΔlogP = 0.80, PSA = 39.1 Å^2) further illustrate the dangers of using PSA or counting hydrogen bonding groups without taking account of hydrogen bond strength.

Measured values of ΔlogP show how hydrogen bond acceptor strength can be modulated by electronic effects. The acceptor strength of quinoline (**3**, ΔlogP = 1.02) appears to be more sensitive to aza-substitution at C4 (**5**, ΔlogP = 0.84) than at C5 (**6**, ΔlogP = 1.28). In the absence of electronic effects, both **5** and **6** would be expected to have a ΔlogP of 2.04, assuming additivity. In contrast, the ΔlogP of **47** (1.75) is much closer to the sum of the ΔlogP values measured for **3** (1.02) and **4** (1.11) that would be expected for independent acceptors. Pyridazine has been observed[32] to be a stronger hydrogen bond acceptor than either pyrazine or pyrimidine and this is believed to be a manifestation of the α-effect[47] in which interactions[32,36] between adjacent lone pairs overcome the effect of a directly bonded electronegative atom. The presence of the second electronegative oxygen atom can be invoked to explain the observation that the ΔlogP for the sulfone **38** (1.65) is significantly less than twice the value measured for the sulfoxide **36** (1.45). While the ΔlogP is greater for the amide **15** (1.68) than for the ketone **14** (0.65), a lower value is observed for the sulfonamide **39** (1.08) than for the sulfone **38** (1.65), reflecting the lack of amide-like resonance in sulfonamides.[48,49]

The ΔlogP value observed (1.31) for the lactone **31** in this study is larger than the value that has been reported (0.51) for its acyclic analogue **56**. A singly connected oxygen atom functioning as a hydrogen bond acceptor typically has a pair of electrostatic potential minimum associated with it, and different values of the electrostatic potential are often observed for these. In this study, electrostatic potentials are quoted in the atomic units[38] of Hartree/electron, and negative values are associated with hydrogen bond acceptors. The minimum associated with the carbonyl oxygen atom can be specified according to their relationship to the other oxygen atom, and for **56**, the anti V_{min} (−0.091) was observed to be more negative than the syn V_{min} (−0.086). While the anti V_{min} (−0.093) for the lactone **31** is very similar to that of **56**, the syn V_{min} (−0.104) is more negative. This can be interpreted as being due to a secondary electrostatic interaction[50] between non-bonded electrons associated with the two oxygen atoms of the lactone. The observation that the V_{min} value associated the doubly connected oxygen of **31** (−0.072) is more negative that the corresponding figure for **56** (−0.054) provides additional evidence for the secondary electrostatic interaction.

Figures 3–5 and the results in Table 3 show that V_{min} is a useful predictor of ΔlogP. Carbonyl oxygen atoms (Figure 4) are associated with larger ΔlogP values for a given V_{min} than nitrogen or ether oxygen atoms (Figure 3). This is probably a consequence of carbonyl oxygen atoms having two minima because only the most negative one is used as a predictor of ΔlogP. As will be shown later, formation of a hydrogen bond between carbonyl oxygen and a donor eliminates one electrostatic potential minimum associated with the oxygen atom and perturbs the other. A consequence of this is that the contributions of the two V_{min} values associated with the oxygen atoms cannot be assumed to be additive.

The observed relationships between ΔlogP and V_{min} have implications for other approaches to modeling hydrogen bonding. Using the RHF model to calculate V_{min} resulted in better fitting of the experimental results across all three acceptor classes than when the B3LYP or MP2 models were used. One should not draw any physical conclusions from the relative performance of the three models because a gas phase electrostatic property, calculated at a single point in space, has been used as a descriptor to model a solution phase phenomenon. The results are consistent with the view that charges fit to electrostatic potential calculated at the RHF/6-31G* level are particularly appropriate for calculation of free energies within a force field paradigm.[51] However, the basis for that view may need to be re-examined for hypervalent species given that ΔlogP values for singly connected oxygen acceptors appear to respond differently to V_{min} depending on whether or not they are bound to a hypervalent atom. Electrostatic potential minima are typically found between 1.2 and 1.3 Å from the relevant oxygen or nitrogen, suggesting that the van der Waals radius may not be especially relevant to hydrogen bonding. The effectiveness of V_{min} as a descriptor of hydrogen bond acceptor strength presents another challenge[52–54] to the use of atom-centered charges to model hydrogen bonding.

While the relationships between ΔlogP and V_{min} are useful in a predictive sense, it is worth posing the question of why this should be the case. Describing hydrogen bond acceptors by single values of calculated electrostatic potential cannot be expected to quantify the entropic component of hydrogen bonding. The observed fits of ΔlogP suggest that V_{min} quantifies the enthalpic component in an effective manner and that the entropic component is either constant or correlated with enthalpy.[55–57] Dunitz has argued[56] that "enthalpy−entropy compensation is a general property of weak intermolecular interactions". While the nonlinear relationship between ΔlogP and V_{min} is consistent with solvent polarization, it may also reflect nonlinear enthalpy−entropy compensation.

Polarization effects are of interest in addressing the issue of hydrogen bond acceptors interacting with more than one donor simultaneously[20] and, more generally, in molecular force field development.[58,59] Results presented in Table 4 quantify the effects of 1−1 complex formation on other hydrogen bond acceptor centers in the system. As might be expected, 1−1 complex formation leads to a reduction in magnitude of the V_{min} value associated with the carbonyl oxygen. This reflects polarization of the acceptor oxygen, which makes the unused lone pair less available for formation of a second hydrogen bond and secondary electrostatic interactions with the donor in the complex. The V_{min} value (−0.114) for the carbonyl oxygen in the complex of **63** with methanol is significantly more negative than the most negative V_{min} values for the tertiary amides **17** (−0.107) and **18** (−0.110), suggesting that this oxygen acceptor will readily form two hydrogen bonds. Complexation of the

weaker acceptor **62** reduces V_{min} to a figure (−0.092), which is virtually identical to that calculated for the ketone **14**. The V_{min} values for methanol oxygen atoms in the complexes are all more negative than the value (−0.096) for an isolated methanol molecule and, as expected, the differences increase with the strength of the hydrogen bond acceptor. The calculations illustrate how the hydrogen bond effectively relays hydrogen bond acceptor potential from carbonyl oxygen to methanol oxygen. One consequence of polarization is that the contribution of a hydroxyl hydrogen bond acceptor to ΔlogP is not expected to be accurately predicted using eq 1a. The value of these calculations is that they bring the effects of intermolecular complexation and structural variation onto the same scale.

While the results presented show that contributions of hydrogen bond acceptors to ΔlogP can be predicted using calculated molecular electrostatic potentials, it is likely that a general method for prediction of this quantity will make use of substructurally defined fragment contributions.[16] Fragment contributions are most applicable where the hydrogen bonding group is isolated electronically from the rest of the molecule as is the case for aliphatic amines and alcohols. For example, our measured values of ΔlogP for **17** (1.76) and **18** (1.92) were used to derive a fragment value of 1.84 for aliphatic tertiary amides. We use two examples to illustrate prediction of ΔlogP from calculated and experimentally derived fragment contributions and show how these predictions can provide insight into central nervous system (CNS) penetration.

The observation that morphine (**64**) crosses the blood−brain barrier less efficiently than its diacetylated analogue diamorphine (**65**) has been presented as a textbook[60,61] example of the effect of lipophilicity on CNS penetration. This observation has been rationalized by noting that in diamorphine there are "two polar groups which are masked"[60] and "because of its greater lipid solubility, it crosses the blood−brain barrier more rapidly than morphine".[61] The measured $logP_{oct}$ values for **64** (0.89) and **65** (1.58) only differ by 0.7 units, and by the PSA metric, **65** (65.1 Å^2) is actually more polar than **64** (52.9Å^2). However the values of $logP_{hxd}$ predicted for **64** (−4.2) and **65** (−1.4) show that diacetylation of **64** leads to a larger increase of almost 3 units in this partitioning system.

Measured brain/blood concentration ratios[41] were used to evaluate the effectiveness of $logP_{hxd}$ as a predictor of CNS penetration. While measurements such as these do not quantify blood−brain barrier permeability directly and also reflect relative binding affinity to plasma proteins and brain tissue,[62,63] they are commonly used to evaluate potential CNS drugs.[6] Our method for predicting contributions to ΔlogP from electrostatic potential is currently restricted to hydrogen bond acceptors, and the only donors that can be treated are those for which measured substructural contributions are available such as hydroxyl groups and secondary amines. Despite this restriction, the 15 basic and 3 neutral compounds in the data set present 12 structural cores and the $\log(C_{brain}/C_{blood})$ values span 3.5 units.

The observation that $logP_{hxd}$ is a more effective predictor of CNS penetration than $logP_{oct}$ for this data set reinforces the view that alkane/water partition coefficients, when accessible, may be more appropriate than their 1-octanol/water equivalents for modeling passive permeability[13] and binding to proteins.[14] It is more difficult to rationalize the advantage ΔlogP appears to have over $logP_{hxd}$ as a predictor of CNS penetration. However, our results do support earlier work in which the former was identified as a descriptor that is particularly suitable for prediction of CNS penetration.[17] Although derived as the difference between logP values for two solvents, ΔlogP approximates to the 1-octanol/hexadecane partition coefficient and that relationship becomes exact when the three mutual solubilities of the solvents are all zero. It is not clear why a partitioning system in which the polar component is 1-octanol should be such an effective predictor of $\log(C_{brain}/C_{blood})$ although binding to plasma proteins and brain tissue may be a factor. Our results and other studies[16,17] suggest ΔlogP is a useful descriptor in its own right that is related to PSA and counts of hydrogen bonding groups while providing a better indication of hydrogen bond strength.

The value of $logP_{hxd}$ of −7 predicted for **82** suggests that for many compounds of interest hydrocarbon/water partition coefficients will not be routinely measurable. This observation highlights the need for predictive methods and suggests that extension of the electrostatic potential methodology to hydrogen bond donors will be useful. The results of this study validate ΔlogP as a target for predictive modeling and demonstrate the value of experimental measurements of this property for prototypical model compounds.

Conclusions

Hexadecane/water and 1-octanol/water partition coefficients have been measured for model compounds, allowing ΔlogP values to be derived for a number of hydrogen bond acceptors that are neutral under normal physiological conditions. It has been shown that minimized electrostatic potential is a useful descriptor for prediction of the contribution of hydrogen bond acceptors to ΔlogP. The observed relationships between ΔlogP and V_{min} appear to be nonlinear and there appear to be no advantages to using the B3LYP or MP2 theoretical models rather than the simpler RHF model when the 6-31G* basis set is used. Minimized electrostatic potential has also been used to quantify the effect of polarization in hydrogen bonded complexes. Predicted $logP_{hxd}$ and ΔlogP were both shown to be more effective molecular descriptors than predicted $logP_{oct}$ for rationalizing and modeling CNS penetration.

Experimental Section

Quoted values for logD are means of at least 3 measurements. Distribution coefficients were determined using a shake-flask technique,[64] using the difference in the aqueous phase concentration of the analyte before and after partitioning to calculate logD (eq 2). Two separate buffer:organic phase partitioning ratios of 100:1 and 1:1 were employed to achieve a dynamic range of 0.5 to 4 and −2 to 2, respectively. A suitable ratio was chosen for each compound based upon an estimate of logP[11] in the appropriate solvent prior to experiment.

A 10 mM sodium phosphate buffer was prepared using Millipore purified water and adjusted to pH 7.4 with 10 M sodium hydroxide. Saturation of buffer solution with 1-octanol or vice-versa was achieved by thorough mixing of both phases in a separating funnel. The phases were allowed to separate for several days before decanting. Saturation of buffer solution with hexadecane or vice-versa was achieved by continuous stirring of the two-phase system overnight to allow efficient mixing of the phases prior to separation. Analyte compounds (ca. 0.6 mg or 1 μL) were dissolved in 12 mL of phosphate buffer saturated with 1-octanol or hexadecane.

After filtration through a glass fiber filter 10 mL (for 1 100:1 ratios) or 3 mL for (for 1:1 ratios) of analyte solution was placed in a graduated centrifuge tube. Excess solution was transferred into an HPLC vial as the "before partitioning solution (BP)". Then 100 μL (for 100:1 ratios) or 3 mL (for 1:1 ratios) of saturated 1-octanol or hexadecane was added to the centrifuge tube before placement on a Thermolyte Varimix platform and mixing at 25 °C, 20 rpm, and a 48° angle for 30 min. After subsequent centrifugation at 3000 rpm for 30 min at 25 °C, an aliquot of the aqueous bottom layer of

the solution was transferred to an HPLC vial as the "after partitioning solution (AP)".

HPLC analysis was carried out on an Agilent 1100 HPLC binary pump and a UV diode array detector. Samples were separated using a Phenomenex Synergi MaxRP column and a 3 min gradient from 95% aqueous ammonium acetate (50 mM) to 100% methanolic ammonium acetate (44 mM) at 1.2 mL min^{-1}. Data acquisition at 220−320 nm and subsequent integration were carried out using Chemstation version 6. Blank injections of buffer, 1-octanol, and DMSO were used to assess background interference from the solvents. A standard solution of the analyte in DMSO was used as a retention time guide for the compound being measured.

The logD result at pH 7.4 is calculated from eq 2 using a Microsoft Excel spreadsheet:

$$\log D = \log \left[\frac{\text{peak area of BP} - \text{peak area of AP}}{\text{peak area of AP}} \times \frac{\text{aqueous volume}}{\text{organic volume}} \right] \quad (2)$$

QC compounds were included in each experimental to ensure analytical reproducibility.

Computational Details

Quantum mechanical calculations were performed using the Gaussian 03 program[65] using the 6-31G* basis set[38] and molecular geometries were energy-minimized at the restricted Hartree−Fock (RHF) level of theory.[38] Starting structures for **16** and **24** were each built with the phenyl ring anti with respect to the carbonyl oxygen, as suggested by crystal structures with refcodes MEACAN10 and YOFDIG in the Cambridge Structural Database.[66] Minimized electrostatic potentials (V_{min}) were calculated using the keyword Prop=(Opt,EFG) for these geometries using RHF, second-order Møller−Plesset perturbation theory (MP2),[38] and Becke three-parameter exchange functional, combined with the Lee−Yang−Parr correlation functional (B3LYP)[39] electronic structure models. In cases where more than one electrostatic potential minimum was found for an atom, the most negative of these was used as the descriptor of hydrogen bond acceptor strength for that atom. All computed electrostatic potentials are quoted in atomic units[38] (Hartree/electron). Values of PSA were calculated from SMILES[67] using the Molinspiration interactive PSA calculator,[68] which is based on the method of Ertl, Rohde, and Selzer.[28]

Nonlinear regression analysis was performed using the JMP statistical program.[69] Atomic contributions to ΔlogP were assumed to be additive, and values used in regression analysis were statistically corrected when equivalent hydrogen bond acceptor atoms were present. Contributions of oxygen and nitrogen atoms to ΔlogP were neglected when these were linked to carbonyl or sulfonyl groups either directly or vinylogously (e.g., **29**, **34**). Other heteroatom contributions that were neglected include hypervalent nitrogen (e.g., nitro), triply connected nitrogen in a heteroaromatic ring (e.g., N1 of **7**), oxygen in an aromatic ring (e.g., **9**), and oxygen in **42**.

Values of ΔlogP for analysis of CNS penetration were predicted using fragment contributions derived from measurements and, when these were not available, by application of eqs 1a (heteroaromatic nitrogen and ether oxygen acceptors) or 1d (carbonyl oxygen acceptors). Fragment contributions ($\Delta\log P_{ss}$) were defined for aliphatic tertiary amide (1.84; this work; mean ΔlogP for **17** and **18**), aliphatic hydroxyl (1.6; mean ΔlogP for 23 aliphatic alcohols[25]), phenolic hydroxyl (2.5; ΔlogP of phenol[25]), alkoxybenzene (0.25; this work; ΔlogP for **12**), secondary aliphatic amine (1.0; mean ΔlogP for 4 secondary amines[25]), and tertiary aliphatic amine (0.8; mean ΔlogP for trimethylamine and triethylamine[25]). The contributions to ΔlogP of dialkylamino nitrogen bound to aromatic carbon and alkylamino nitrogen bound to two aromatic carbon atoms were neglected on the basis of the similarity of measured values of $\log P_{oct}$ (2.31[42]) and $\log P_{hxd}$ (2.22[24]) reported for *N*,*N*-dimethylaniline. Self-association in hexadecane was neglected when deriving $\Delta\log P_{ss}$ contributions for hydroxyl groups and secondary amines. Values of $\Delta\log P_{mep}$ were calculated using the most prototypical member of series of closely related compounds: **71** (represents **70** and **71**), **73** (represents **72** and **73**), **76** (represents **76** and **77**), and **80** (represents **80**, **81**, **82**). Predicted $\log P_{hxd}$ values were generated as the difference of *C*logP[11] and $\Delta\log P_{pred}$.

Acknowledgment. We thank Andrew G. Leach and the two anonymous reviewers for helpful and insightful comments on the manuscript.

Supporting Information Available: Coordinates for energy-minimized structures are provided. This material is available free of charge via the Internet at http://pubs.acs.org.

References

(1) Lipinski, C. A.; Lombardo, F.; Dominy, B. W.; Feeney, P. J. Experimental and computational approaches to estimate solubility and permeability in drug discovery and development settings. *Adv. Drug Delivery Rev.* **1997**, *23*, 3–25.
(2) van de Waterbeemd, H.; Smith, D. A.; Beaumont, K.; Walker, D. K. Property-based design: Optimization of drug absorption and pharmacokinetics. *J. Med. Chem.* **2001**, *44*, 1–21.
(3) Avdeef, A. Physicochemical profiling (solubility, permeability and charge state). *Curr. Top. Med. Chem.* **2001**, *1*, 277–351.
(4) Fujita, T.; Iwasa, J.; Hansch, C. A new substituent constant, π, derived from partition coefficients. *J. Am. Chem. Soc.* **1964**, *86*, 5175–5180.
(5) Avdeef, A.; Bendels, S.; Di, L.; Faller, B.; Kansy, M.; Sugano, K.; Yamauchi, Y. Parallel artificial membrane permeability assay (PAMPA)-critical factors for better predictions of absorption. *J. Pharm. Sci.* **2007**, *96*, 2893–2909.
(6) Hitchcock, S. A.; Pennington, L. D. Structure−brain exposure relationships. *J. Med. Chem.* **2006**, *49*, 7559–7583.
(7) Lombardo, F.; Obach, R. S.; Shalaeva, M. Y.; Gao, F. Prediction of volume of distribution values in humans for neutral and basic drugs using physicochemical measurements and plasma protein binding data. *J. Med. Chem.* **2002**, *45*, 2867–2876.
(8) Delaney, J. S. Predicting aqueous solubility from structure. *Drug Discovery Today* **2005**, *10*, 289–295.
(9) Ran, Y.; Yalkowsky, S. H. Prediction of drug solubility by the general solubility equation (GSE). *J. Chem. Inf. Comput. Sci.* **2001**, *41*, 354–357.
(10) Jamieson, C. M. J.; Moir, E. M.; Rankovic, Z.; Wishart, G. Medicinal chemistry of hERG optimizations: Highlights and hang-ups. *J. Med. Chem.* **2006**, *49*, 5029–5045.
(11) *C*log*P*, BioByte Corp., 201 W 4th Street, no. 204, Claremont CA 91711−4707; http://www.biobyte.com
(12) Dallas, A. J.; Carr, P. W. A thermodynamic and solvatochromic investigation of the effect of water on the phase-transfer properties of octan-1-ol. *J. Chem. Soc., Perkin Trans. 2* **1992**, 2155–2161.
(13) Mayer, P. T.; Anderson, B. T. Transport across 1,9-decadiene precisely mimics the chemical selectivity of the barrier in egg Lecithin bilayers. *J. Pharm. Sci.* **2002**, *91*, 640–646.
(14) Wolfenden, R. Experimental measures of amino acid hydrophobicity and the topology of transmembrane and globular proteins. *J. Gen. Physiol.* **2007**, *129*, 357–362.
(15) Fujii, Y.; Sobue, K.; Tanaka, M. Solvent effect on the dimerization and hydration constant of benzoic acid. *J. Chem. Soc., Faraday Trans. 1* **1978**, *74*, 1467–1476.
(16) Seiler, P. Interconversion of lipophilicities from hydrocarbon/water systems into the octanol/water system. *Eur. J. Med. Chem.* **1974**, *9*, 473–479.
(17) Young, R. C.; Mitchell, R. C.; Brown, T. H.; Ganellin, C. R.; Griffiths; Jones, R. M.; Rana, K. K.; Saunders, D.; Smith, I. R.; Sore, N.; Wilks, T. J. Development of a new physicochemical model for brain penetration and its application to the design of centrally acting H2 receptor histamine antagonists. *J. Med. Chem.* **1988**, *31*, 656–671.
(18) Goodwin, J. T.; Conradi, R. A.; Ho, N. F. H.; Burton, P. S. Physicochemical determinants of passive membrane permeability: role of solute hydrogen-bonding potential and volume. *J. Med. Chem.* **2001**, *44*, 3721–3729.
(19) Leahy, D. E.; Morris, J. J.; Taylor, P. J.; Wait, A. R. Model solvent systems for QSAR. Part 2. Fragment values (f-values) for the critical quartet. *J. Chem. Soc. Perkin Trans. 2* **1992**, 723–731.

(20) Leahy, D. E.; Morris, J. J.; Taylor, P. J.; Wait, A. R. Model solvent systems for QSAR. Part 3. An LSER analysis of the critical quartet. New light on hydrogen bond strength and directionality. *J. Chem. Soc. Perkin Trans. 2* **1992**, 705–722.

(21) Leahy, D. E.; Morris, J. J.; Taylor, P. J.; Wait, A. R. Model solvent systems for QSAR. Part IV. The Hydrogen Bond Acceptor Behaviour of Heterocycles. *J. Phys. Org. Chem.* **1994**, *7*, 743–750.

(22) Riebesehl, W.; Tomlinson, E.; Gruenbauer, H. J. M. Thermodynamics of solute transfer between alkanes and water. *J. Phys. Chem.* **1984**, *88*, 4775–4779.

(23) Abraham, M. H.; Grellier, P. L.; McGill, R. A. Determination of olive oil−gas and hexadecane−gas partition coefficients, and calculation of the corresponding olive oil−water and hexadecane−water partition coefficients. *J. Chem. Soc., Perkin Trans. 2* **1987**, 797–803.

(24) Abraham, M. H.; Whiting, G. S.; Fuchs, R. J.; Chambers, E. J. Thermodynamics of solute transfer from water to hexadecane. *J. Chem. Soc., Perkin Trans. 2* **1990**, 291–300.

(25) Abraham, M. H.; Chadha, H. S.; Whiting, G. S.; Mitchell, R. C. Hydrogen bonding. 32. An analysis of water−octanol and water−alkane partitioning and the ΔlogP parameter of Seiler. *J. Pharm. Sci.* **1994**, *83*, 1085–1100.

(26) Tsai, R. S.; Fan, W.; El Tayar, N.; Carrupt, P. A; Testa, B.; Kier, L. B. Solute−water interactions in the organic phase of a biphasic system. 1. Structural influence of organic solutes on the "water-dragging" effect. *J. Am. Chem. Soc.* **1993**, *115*, 9632–9639.

(27) Palm, K.; Luthman, K.; Ungell, A.-L.; Strandlund, G.; Artursson, P. Correlation of drug absorption with molecular surface properties. *J. Pharm. Sci.* **1996**, *85*, 32–39.

(28) Ertl, P.; Rohde, B.; Selzer, P. Fast calculation of molecular polar surface area as a sum of fragment-based contributions and its application to the prediction of drug transport properties. *J. Med. Chem.* **2000**, *43*, 3714–3717.

(29) Labute, P. A widely applicable set of descriptors. *J. Mol. Graph. Model.* **2000**, *18*, 464–477.

(30) Abraham, M. H. Scales of solute hydrogen-bonding: their construction and application to physicochemical and biochemical processes. *Chem. Soc. Rev.* **1993**, *22*, 73–83.

(31) Laurence, C.; Berthelot, M. Observations on the strength of hydrogen bonding. *Perspect. Drug Discovery Des.* **2000**, *18*, 39–60.

(32) Abraham, M. H.; Duce, P. D.; Prior, D. V.; Barratt, D. G.; Morris, J. J.; Taylor, P. J. Hydrogen bonding: part 9. Solute proton donor and proton acceptor scales for use in drug design. *J. Chem. Soc., Perkin Trans. 2* **1998**, 1355–1375.

(33) Abraham, M. H.; Ibrahim, A.; Zissimos, A. M.; Zhao, Y. H.; Comer, J.; Reynolds, D. P. Application of hydrogen bonding calculations in property based drug design. *Drug Discovery Today* **2002**, *7*, 1056–1063.

(34) Murray, J. S.; Politzer, P. Relationships between solute hydrogen-bond acidity/basicity and the calculated electrostatic potential. *J. Chem. Res. S.* **1992**, *3*, 110–111.

(35) Murray, J. S.; Raganathan, S.; Politzer, P. Correlations between the solvent hydrogen bond acceptor parameter β and the calculated molecular electrostatic potential. *J. Org. Chem.* **1991**, *56*, 3734–3739.

(36) Kenny, P. W. Prediction of hydrogen bond basicity from computed molecular electrostatic properties: Implications for comparative molecular field analysis. *J. Chem. Soc., Perkin Trans. 2* **1994**, 199–202.

(37) Perrin, D. D. *Dissociation constants of organic bases in aqueous solution: Supplement 1972*; Butterworths: London, 1972.

(38) Szabo, A.; Ostlund, N. S. *Modern Quantum Chemistry. Introduction to Advanced Electronic Structure Theory*; Dover: Mineola, NY, 1996.

(39) Koch, W.; Holthausen, M. C. *A Chemist's Guide to Density Functional Theory*; Wiley-VCH Verlag GmbH & Co.: Weinhem, 2000.

(40) Avdeef, A.; Barrett, D. A.; Shaw, P. N.; Knaggs, R. D.; Davis, S. S. Octanol−, chloroform−, and propylene glycol dipelargonate−water partitioning of morphine-6-glucuronide and other related opiates. *J. Med. Chem.* **1996**, *39*, 4377–4381.

(41) Kelder, J.; Grootenhuis, P. D. J.; Bayada, D. M.; Delbressine, L. P. C.; Ploemen, J.-P. Polar molecular surface as a dominating determinant for oral absorption and brain penetration of drugs. *Pharm. Res.* **1999**, *16*, 1514–1519.

(42) Hansch, C.; Leo, A.; Hoekman; D. *Exploring QSAR Hydrophobic, Electronic, and Steric Constants*; American Chemical Society: Washington DC, 1995.

(43) Zwanzig, R. W. High-temperature equation of state by a perturbation method. I. Nonpolar gases. *J. Chem. Phys.* **1954**, *22*, 1420–1426.

(44) Kenny, P. W.; Sadowski, J. Structure Modification in Chemical Databases. In *Chemoinformatics in Drug Discovery*; Oprea, T. I., Ed.; Wiley-VCH Verlag GmbH & Co.: Weinheim, 2005; Vol. 23, pp 271−284.

(45) Leach, A. G.; Jones, H. D.; Cosgrove, D. A.; Kenny, P. W.; Ruston, L.; MacFaul, P.; Wood, J. M.; Colclough, N.; Law, B. Matched molecular pairs as a guide in the optimization of pharmaceutical properties; A study of aqueous solubility, plasma protein binding and oral exposure. *J. Med. Chem.* **2006**, *49*, 6672–6682.

(46) Jiménez-Lozano, E.; Marqués, I.; Barrón, D.; Beltrán, J. L.; Barbosa, J. Determination of pK_a values of quinolones from mobility and spectroscopic data obtained by capillary electrophoresis and a diode array detector. *Anal. Chim. Acta* **2002**, *464*, 37–45.

(47) Edwards, J. O.; Pearson, R. G. The Factors Determining Nucleophilic Reactivities. *J. Am. Chem. Soc.* **1962**, *84*, 16–24.

(48) Wood, J. M.; Page, M. I. The mechanisms of sulfonyl transfer in strained cyclic sulfonamides. *Trends Heterocycl. Chem.* **2002**, *8*, 19–34.

(49) Chardin, A.; Laurence, C.; Berthelot, M.; Morris, D. G. Hydrogen-bond basicity of the sulfonyl group. The case of strongly basic sulfonamidates $RSO_2N^-N^+Me_3$. *J. Chem. Soc., Perkin Trans. 2* **1996**, 1047–1051.

(50) Jorgensen, W. L.; Pranata, J. Importance of secondary interactions in triply hydrogen bonded complexes: guanine-cytosine vs uracil-2,6-diaminopyridine. *J. Am. Chem. Soc.* **1990**, *112*, 2008–2010.

(51) Jakalian, A.; Bush, B. L.; Jack, D. B.; Bayly, C. I. Fast, efficient generation of high-quality atomic charges. AM1-BCC model: I. Method. *J. Comput. Chem.* **2000**, *21*, 132–146.

(52) Day, G. M.; Motherwell, W. D. S.; Jones, W. Beyond the Isotropic Atom Model in Crystal Structure Prediction of Rigid Molecules: Atomic Multipoles versus Point Charges. *Cryst. Growth Des.* **2005**, *5*, 1023–1033.

(53) Rasmussen, T. D.; Ren, P.; Ponder, J. W.; Jensen, F. Force field modeling of conformational energies: importance of multipole moments and intramolecular polarization. *Int. J. Quantum Chem.* **2007**, *107*, 1390–1395.

(54) Cheeseright, T.; Mackey, M.; Rose, S.; Vinter, A. Molecular field extrema as descriptors of biological activity: Definition and validation. *J. Chem. Inf. Mod.* **2006**, *46*, 665–676.

(55) Sharp, K. Entropy-enthalpy compensation: fact or artifact? *Protein Sci.* **2001**, *10*, 661–667.

(56) Dunitz, J. D. Win some, lose some: Enthalpy−entropy compensation in weak intermolecular interactions. *Chem. Biol.* **1995**, *2*, 709–712.

(57) Lumry, R.; Rajender, S. Enthalpy−entropy compensation phenomena in water solutions of proteins and small molecules: A ubiquitous property of water. *Biopolymers* **1970**, *9*, 1125–1227.

(58) Maple, J. R.; Cao, Y.; Damm, W.; Halgren, T. A.; Kaminski, G. A.; Zhang, L. Y.; Friesner, R. A. A polarizable force field and continuum solvation methodology for modeling of protein−ligand interactions. *J. Chem. Theory Comput.* **2005**, *1*, 694–715.

(59) Xie, W.; Pu, J.; MacKerell, A. D.; Gao, J. Development of a polarizable intermolecular potential function (PIPF) for liquid amides and alkanes. *J. Chem. Theory Comput.* **2007**, *3*, 1878–1889.

(60) Patrick, G. L. *An Introduction to Medicinal Chemistry*, 3rd ed.; Oxford University Press: Oxford, 2005, pp 620.

(61) Rang, H. P.; Dale, M. M.; Ritter, J. M. *Pharmacology*, 4th ed.; Churchill Livingstone: Edinburgh, 1999; pp 598.

(62) Summerfield, S. G.; Stevens, A. J.; Cutler, L.; Osuna, M. D. C.; Hammond, B.; Tang, S.-P.; Hersey, A.; Spalding, D. J.; Jeffrey, P. Improving the in vitro prediction of in vivo central nervous system penetration: integrating permeability, P-glycoprotein efflux, and free fractions in blood and brain. *J. Pharmacol. Exp. Ther.* **2006**, *316*, 1282–1290.

(63) Kalvass, J. C.; Maurer, T. S.; Pollack, G. M. Use of plasma and brain unbound fractions to assess the extent of brain distribution of 34 drugs: comparison of unbound concentration ratios to in vivo P-glycoprotein efflux ratios. *Drug Metab. Dispos.* **2007**, *35*, 660–666.

(64) Dearden, J. C.; Bresnen, G. M. The measurement of partition coefficients. *Quant. Struct.−Act. Relat.* **1988**, *7*, 133–144.

(65) Frisch, M. J.; Trucks, G. W.; Schlegel, H. B.; Scuseria, G. E.; Robb, M. A.; Cheeseman, J. R.; Montgomery, J. A., Jr.; Vreven, T.; Kudin, K. N.; Burant, J. C.; Millam, J. M.; Iyengar, S. S.; Tomasi, J.; Barone, V.; Mennucci, B.; Cossi, M.; Scalmani, G.; Rega, N.; Petersson, G. A.; Nakatsuji, H.; Hada, M.; Ehara, M.; Toyota, K.; Fukuda, R.; Hasegawa, J.; Ishida, M.; Nakajima, T.; Honda, Y.; Kitao, O.; Nakai, H.; Klene, M.; Li, X.; Knox, J. E.; Hratchian, H. P.; Cross, J. B.; Bakken, V.; Adamo, C.; Jaramillo, J.; Gomperts, R.; Stratmann, R. E.; Yazyev, O.; Austin, A. J.; Cammi, R.; Pomelli, C.; Ochterski, J. W.; Ayala, P. Y.; Morokuma, K.; Voth, G. A.; Salvador, P.; Dannenberg, J. J.; Zakrzewski, V. G.; Dapprich, S.; Daniels, A. D.; Strain, M. C.; Farkas, O.; Malick, D. K.; Rabuck, A. D.; Raghavachari, K.; Foresman, J. B.; Ortiz, J. V.; Cui, Q.; Baboul, A. G.; Clifford, S.; Cioslowski, J.; Stefanov, B. B.; Liu, G.; Liashenko, A.; Piskorz, P.; Komaromi, I.; Martin, R. L.; Fox, D. J.; Keith, T.; Al-Laham, M. A.; Peng, C. Y.; Nanayakkara, A.; Challacombe, M.; Gill, P. M. W.; Johnson, B.; Chen, W.; Wong, M. W.; Gonzalez, C.; Pople, J. A. *Gaussian 03*, revision B.05; Gaussian, Inc.: Wallingford, CT, 2004; http://www.gaussian.com.

(66) Cambridge Structural Database, Cambridge Crystallographic Data Centre, 12 Union Road, Cambridge CB2 1EZ, UK; http://www.ccdc.cam.ac.uk/products/csd/.
(67) Weininger, D. SMILES, a chemical language and information system. 1. Introduction to methodology and encoding rules. *J. Chem. Inf. Comput. Sci.* **1988**, *28*, 31–36.
(68) Property calculation engine mib v2007.04, Molinspiration; http://www.molinspiration.com.
(69) JMP Version 6.0.0, SAS Institute, SAS Campus Drive, Building S, Cary, NC 27513; http://www.jmp.com.

JM701549S